



ISSN: 0067-2904

## Study of the Nuclear Structure of Positron-Emitting Nuclides for Use in Medical Diagnosis

R. A. Radhi

Department of Radiology Techniques, Al-Hadi University College, Baghdad, Iraq

Received: 14/12/2022 Accepted: 11/10/2023 Published: 10/9/2024

### Abstract

Study of the nuclear structure of nuclides used for medical diagnosis using positron emission tomography (PET) is presented in this work. These nuclides are  $^{11}\text{C}$ ,  $^{13}\text{N}$ ,  $^{15}\text{O}$  and  $^{18}\text{F}$ , which are unstable by emitting  $\beta^+$  particles. They have half-lives of several minutes, which make them suitable radionuclides for PET. These radionuclides are produced through nuclear reactions using a cyclotron. Studying the nuclear structure of these light nuclides is performed through the shell model. The full space of the  $p$ -shell model is used for the  $p$ -shell nuclei, and the full space of the  $sd$ -shell model for the  $sd$ -shell nucleus. The study includes calculations of magnetic moments and quadrupole electric moments. Calculations of form factors are presented to give predictions for future experimental studies. Protons and neutrons' effective charges are used to include core-polarization effects. The single-particle states used in the calculations are those of the harmonic oscillator potential. Excellent agreement is obtained between the calculated observables and the available experimental data.

**Keywords:** Nuclear shell model; Quadrupole moments, Magnetic moments; Elastic form factors; Nuclides used in Positron emission tomography.

### دراسة التركيب النووي للنويدات التي تنبعث منها البوزيترونات للاستخدام في التشخيص الطبي

رعد عبد الكريم راضي

قسم تقنيات الاشعة, كلية الهادي الجامعة, بغداد 10011 العراق

### الخلاصة

دراسة التركيب النووي للنويدات المستخدمة في التشخيص الطبي باستخدام التصوير المقطعي بالإصدار البوزيتروني (PET). هذه النويدات هي  $^{15}\text{O}$ ,  $^{13}\text{N}$ ,  $^{11}\text{C}$  و  $^{18}\text{F}$  وهي غير مستقرة عن طريق انبعاث جسيمات  $\beta^+$ . نصف العمر لهذه النويدات هو عدة دقائق مما يجعلها نويدات مشعة ملائمة للتصوير المقطعي بالإصدار البوزيتروني. يتم إنتاج هذه النويدات المشعة من خلال التفاعل النووي باستخدام السيكلوترون. تتم دراسة التركيب النووي لهذه النويدات الخفيفة من خلال نموذج القشرة. يتم استخدام فضاء نموذج القشرة  $p$  الكامل للنوى الواقعة ضمن القشرة  $p$ -shell، والتي هي  $^{13}\text{N}$ ,  $^{11}\text{C}$  و  $^{15}\text{O}$ ، وفضاء نموذج القشرة  $sd$  الكامل لنواة  $^{18}\text{F}$  التي تقع ضمن القشرة  $sd$ . تتضمن الدراسة حسابات العزوم المغناطيسية و عزوم رباعي القطب الكهربائية. يتم تقديم حسابات عوامل الشكل لإعطاء تنبؤات للدراسات التجريبية المستقبلية. تستخدم الشحنات الفعالة للبروتونات وللنيوترونات لتشمل تأثيرات استقطاب القلب. حالات الجسيم الواحد المستخدمة في

الحسابات هي حالات جهد المذبذب التوافقي. تم الحصول على اتفاق ممتاز بين المعطيات المحسوبة والبيانات التجريبية المتاحة.

## 1. Introduction

Coulomb C2 form factors for some  $p$ -shell nuclei have been studied [1], where experimental data are available. Their calculations include core polarization effect, and it was found that this effect must be included to explain the experimental results of the transition strengths  $B(E2)$  values and momentum transfer dependence of form factors. Nuclear structure studies have been performed for  $p$ -shell nuclei [2] using extended model space with  $2\omega$ . Longitudinal inelastic electron scattering form factors have been studied [3] for  ${}^{6,7}\text{Li}$ , by extending the calculations to include  $4\omega$ . Their results were not able to describe the low momentum transfer form factors; besides, the  $B(E2)$  values were underestimated by a factor of 2. Core-polarization effects were adopted through microscopic model [4] to study the Coulomb electron scattering form factors for  ${}^6\text{Li}$ , where the data are very well described. Calculations of  $B(E2)$  values and quadrupole moments for  $A=7$   $p$ -shell nucleus, using large model space up to  $6\omega$ , and for  $A=8-11$   $p$ -shell nuclei using up to  $4\omega$  [5], could not reproduce the experimental data without using effective charges for the protons and neutrons. Using large  $(0 + 2)\omega$  truncated  $spdpf$  model space failed to reproduce the experimental  $B(E2)$  values and elastic and inelastic form factors of  ${}^9\text{Be}$  [6] without taking the excitations from all the orbits in this large model space into all higher orbits up to  $10\omega$ . These calculations give only around 60% of the total matrix elements, while the higher energy configurations (core-polarization effects) give about 40%.

Large basis calculations for Li and B isotopes give effective charges [7] less than the standard effective charges. Electric transition strengths  $B(E2)$  of some even-even neon isotopes have been studied in the  $sd$ -shell model space [8]. Low elastic and inelastic electron scattering form factors have been analyzed [9] for different states in  ${}^9\text{F}$  nucleus. Effective charges are deduced from microscopic calculations for some of Si, S, and Ar isotopes [10]. The calculations are based on the  $sd$  and  $sdpf$ -shell model spaces. Quadrupole moments have been calculated for some Ni isotopes in  $p$  and  $psd$  model spaces [11].

Energy levels, transition rates and electron scattering form factors have been calculated for different states in  ${}^{17}\text{O}$  [12].

In this work, calculations are performed for magnetic dipole moments, electric quadrupole moments and elastic electron scattering for  ${}^{11}\text{C}$ ,  ${}^{13}\text{N}$ ,  ${}^{15}\text{O}$  and  ${}^{18}\text{F}$  nuclides which are unstable by emitting  $\beta^+$  particle that are used in positron emission tomography. Effective charges  $1.35e$  and  $1.45e$  are used in these calculations.

## 2. Theory

The matrix element (ME) of an operator  $\hat{O}$  between nuclear states for a given multipolarity  $\lambda$  is expanded in terms of the single-particle states  $k_a$  and  $k_b$ , as [13]:

$$\langle f || \hat{O}(\lambda) || i \rangle = \sum_{k_a k_b} \langle k_a || \hat{O}(\lambda) || k_b \rangle \text{OBDM}(f i k_a k_b \lambda) \quad (1)$$

where the OBDM is density matrix for one-body states.

The magnetic moment for  $\lambda=1$  is defined in terms of the magnetic matrix element, as in Ref. [14, 13], with  $J_i=J_f$ :

$$\mu = \sqrt{\frac{4\pi}{2\lambda+1}} (J_i \lambda J_f - J_i 0 J_f) \langle f || \hat{O}(M, \lambda) || i \rangle \quad (2)$$

and the one-body magnetic operator is defined as:

$$\hat{O}(M, \lambda, m) = \mu_N \left[ g_s \vec{S} + \left( \frac{2g_l}{\lambda+1} \right) \vec{l} \right] \vec{\nabla} r^\lambda Y_{\lambda\lambda m} \quad (3)$$

The quadrupole moment is defined for  $\lambda=2$ , in terms of the electric matrix element with  $J_i=J_f$ , as:

$$Q = 2 \sqrt{\frac{4\pi}{2\lambda+1}} (J_i \lambda J_f - J_i 0 J_f) \langle f || \hat{O}(E, \lambda) || i \rangle \quad (4)$$

and the one-body electric operator is defined as:

$$\hat{O}(E, \lambda, m) = e r^\lambda Y_{\lambda\lambda m} \quad (5)$$

Form factor for electron scattering is given in terms of the momentum transfer  $q$  as, in Ref. [15], with  $J_i=J_f$ :

$$|F(q, \lambda)|^2 = \left| \frac{1}{Z} \sqrt{\frac{4\pi}{2J_i+1}} \langle f || \hat{T}(M/C, \lambda, q) || i \rangle \right|^2 \quad (6)$$

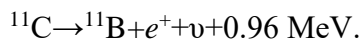
where,  $\hat{T}(M/C, \lambda, q)$  is the magnetic (M)/Coulomb (C) electron scattering operator, given in Ref. [15].

### 3. Results and Discussion

Calculations for  $p$ -shell nuclei, Cohen-Kurath (CKI) interaction [16] was used, while for  $sd$ -shell nucleus, USDA interaction [17] was used. NuShellX@MSU [18] code was adopted to get the OBDM. The size parameter for the harmonic oscillator (HO) potential was obtained from the global formula given in Ref. [19]. The  $Q$  moments and the C2 form factors were calculated with standard effective charges  $e_p=1.35e$ ,  $e_n=0.45e$  [20]. No experimental values are available for the isotopes presented in this work. The form factors were compared with those of the corresponding stable nuclei. All calculated and measured values for the dipole and quadrupole moments for nuclides in this study are given in Table I.

#### 3.1 $^{11}\text{C}$ ( $3/2^-$ )

Carbon-11 is an artificial radioactive isotope with ground state  $J^\pi=3/2^-$ , and decays to Boron-11, which occurs mainly through positron emission  $\beta^+$  (99.79%):



The positron is emitted with an energy equal to 0.96 MeV. As the positron is produced, it annihilates with an electron, producing two gamma rays, each with about 0.511 MeV. These gamma rays are detected by a PET scanner. The half-life of carbon-11 is 20.3 min. Carbon-11 is produced by the bombardment of nitrogen gas by a proton [21] using a cyclotron. Calculation of the magnetic moment for  $3/2^-$  ground state of  $^{11}\text{C}$  gives a value of -0.7832 nuclear magneton (n.m). This value predicted the correct sign as the measured value [22] and close to it (Table I). Calculation of the  $Q$  moment gives a value equal to  $3.352 \text{ efm}^2$  with a positive sign (prolate), while the sign of the experimental value is undetermined. Both predicted and experimental values are close, as given in Table I. The calculations of elastic M1 and C2 form factors are depicted in Figure 1. The corresponding stable nucleus is  $^{13}\text{C}$  ( $1/2^-$ ). The contribution to the elastic electron scattering is M1. No C2 contribution is allowed. So, the M1 contributions of both isotopes are presented in Figure 1 as a small dashed curve for  $^{11}\text{C}$  and a long dashed curve for  $^{13}\text{C}$ . Both calculated M1 form factors are close to each other for all momentum transfer values considered in this work.

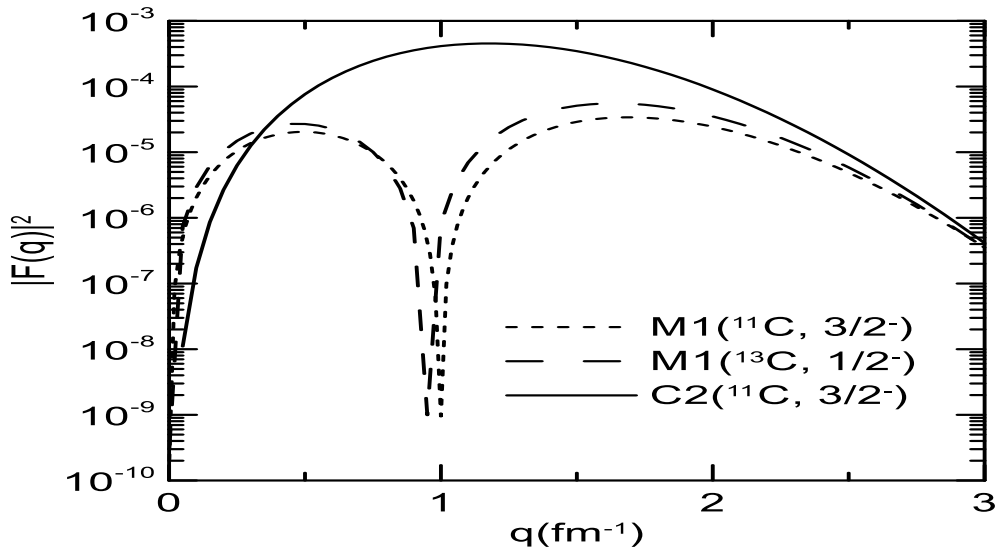
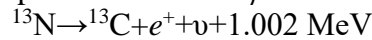


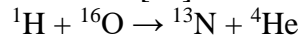
**Figure-1:** Coulomb C2 and M1 elastic electron scattering form factors for the  $3/2^-$  ground state in  $^{11}\text{C}$ . The M1 form factor of the  $3/2^-$  ground state in  $^{11}\text{C}$  is compared with that of  $1/2^-$  ground state in  $^{13}\text{C}$ .

### 3.2 $^{13}\text{N}$ ( $1/2^-$ )

Nitrogen-13 is an artificial radioactive isotope with ground state  $J^\pi = 1/2^-$ , and decays to  $^{13}\text{C}$ , which occurs mainly through positron emission  $\beta^+$ :



The positron is emitted with an energy equal to 1.002 MeV. As the positron is produced, it annihilates with an electron, producing two gamma rays, each with about 0.511 MeV. These gamma rays are detected by a PET scanner. The half-life of nitrogen-13 is about 10 min. Nitrogen-13 is produced in a nuclear reaction [23]:



The proton must be accelerated in a cyclotron to have total energy greater than 5.66 MeV. The theoretical magnetic moment, in this case, reproduces the experimental value [22] very well, as given in Table I. The theoretical predictions were assigned with a negative sign. The sign of the experimental values is not assigned. Calculations of elastic M1 form factors are depicted in Figure 2. The corresponding stable nucleus is  $^{15}\text{N}$  ( $1/2^-$ ). The contribution to the elastic electron scattering is M1. The M1 contributions of both isotopes are presented in Figure 2 as a solid curve for  $^{13}\text{N}$  and a dashed curve for  $^{15}\text{N}$ . Both calculated M1 form factors are close to each other from all momentum transfer values.

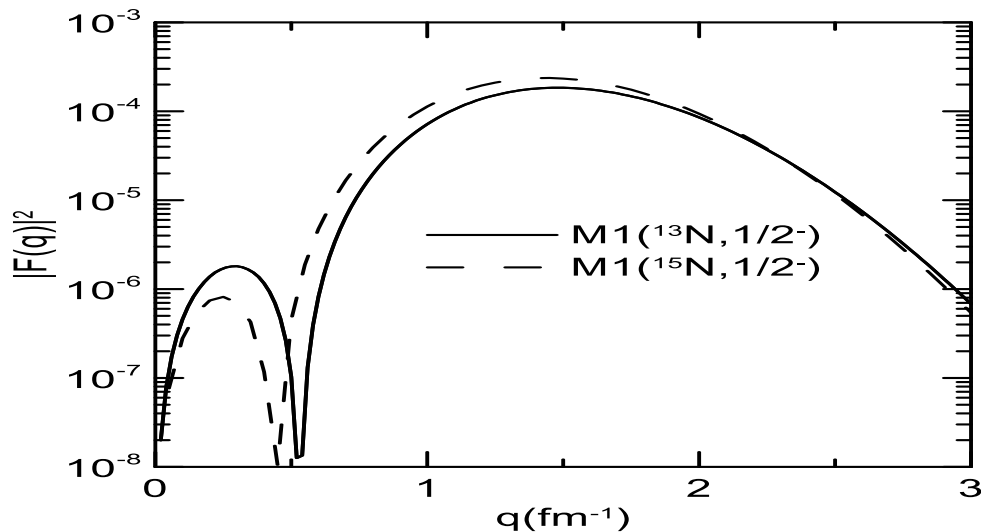
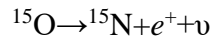


**Figure 2:** Magnetic M1 elastic form factors for the  $1/2^-$  ground state in  $^{13}\text{N}$  and  $^{15}\text{N}$ .

### 3.3 $^{15}\text{O}$ ( $1/2^-$ )

Oxygen-15 is an artificial radioactive isotope with ground state  $J^\pi = 1/2^-$ , and decays to N-15, which occurs mainly through positron emission  $\beta^+$ :



The positron is emitted with an energy equal to 1.002 MeV. As the positron is produced, it annihilates with an electron, producing two gamma rays, each with about 0.511 MeV. These gamma rays are detected by a PET scanner. The half-life of oxygen-15 is about 2 min. Oxygen-15 is produced through the bombardment of  $^{14}\text{N}$  with deuteron using a cyclotron:



The theoretical magnetic moment, in this case, reproduces the experimental value [23] very well, as given in Table I. The theoretical predictions are assigned with a positive sign. The experimental values are not assigned. For this model space, only the active five neutrons contribute, while all protons form a closed inert shell. The predicted M1 form factor is depicted in Figure 3. The corresponding stable isotope is  $^{17}\text{O}$  ( $1/2^+$ ). The M1 form factors for both nuclei are presented in Figure 3 as a solid curve for  $^{15}\text{O}$  and a dashed curve for  $^{17}\text{O}$ . The model space for  $^{15}\text{O}$  is different from that of  $^{17}\text{O}$ . The results are shown in Figure 3. The two form factors are different in shape and magnitude due to the different model spaces. In  $^{17}\text{O}$ , only one active neutron in  $1d_{5/2}$  orbit contributes to the scattering, while for  $^{15}\text{O}$ , one neutron-hole in  $1p_{1/2}$  contributes to the scattering.

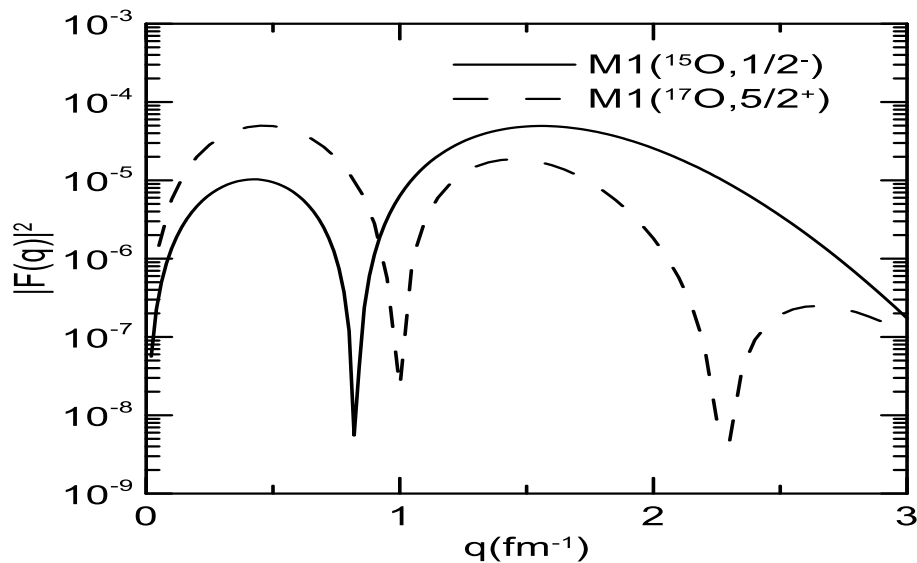
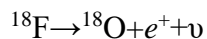


**Figure 3:** Magnetic M1 elastic form factors for the  $1/2^-$  ground state in  $^{15}\text{O}$ , and for the  $5/2^+$  ground state in  $^{17}\text{O}$ .

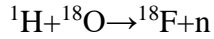
### 3.4 $^{18}\text{F}$ ( $1^+$ )

Of the unstable nuclides of fluorine,  $^{18}\text{F}$  has the longest half-life, about 110 min. Most of the time (96%), the decay mode is by positron emission, while 4% of the time, by electron capture. Stable oxygen-18 is yielded from these two modes of decay. For this reason,  $^{18}\text{F}$  is a commercially important source of positrons:



The positron is emitted with an energy equal to 1.002 MeV. As the positron is produced, it annihilates with an electron, producing two gamma rays, each with about 0.511 MeV. These gamma rays are detected by a PET scanner.

When a proton with 14 MeV, produced from a cyclotron, bombards a stable  $^{18}\text{O}$ ,  $^{18}\text{F}$  is produced.



Fluorine-18 is a doubly open-shell nucleus. Full *sd*-shell calculations with one proton and one neutron are distributed in *sd*-shell orbits. The results of C2 and M1 form factors are depicted in Figure 4, as solid and small dashed curves, respectively. The M1 form factor shows an intermediate maximum, which agrees with the behavior of the M1 form factor of  $^{19}\text{F}$  [9], where the calculated form factor agrees with the experimental data. The M1 form factor of  $^{18}\text{F}$  is an order of magnitude less than that of  $^{19}\text{F}$  at the maximum due to the contribution of one more neutron than those of  $^{18}\text{F}$ .

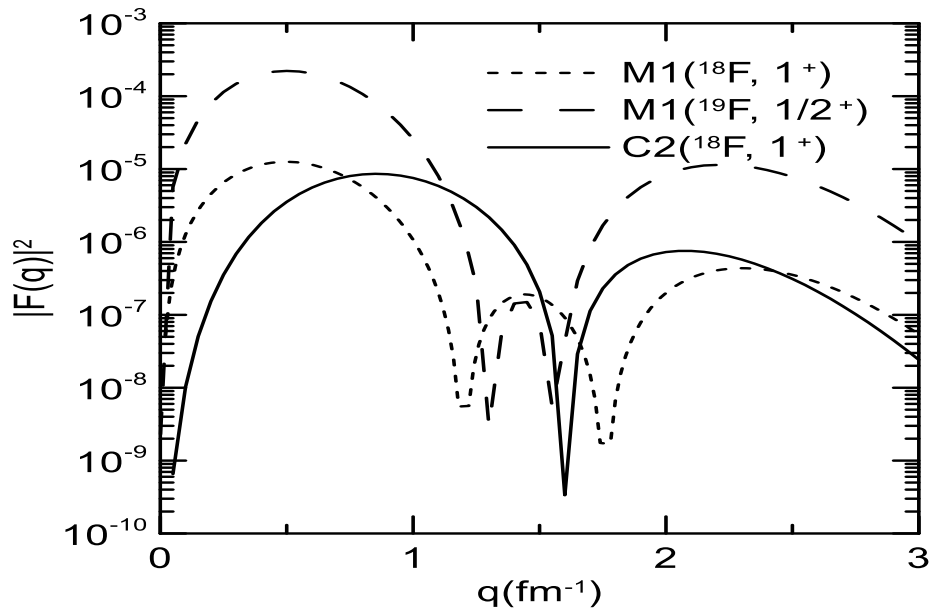


**Figure 4:** Coulomb C2 and M1 elastic electron scattering form factors for the  $1^+$  ground state in  $^{18}\text{O}$ . The M1 form factor of the  $1^+$  ground state in  $^{18}\text{O}$  is compared with that of  $1/2^+$  ground state in  $^{19}\text{O}$ .

**Table 1:** Theoretical and experimental magnetic moments and quadrupole moments. The available experimental values are taken from reference [22].

Nuclide	Half life	$J^\pi$	$B(\text{fm})$	$\mu(\text{nm})_{\text{Theo}}$	$\mu(\text{nm})_{\text{Exp}}$	$Q(\text{efm}^2)_{\text{Theo}}$	$Q(\text{efm}^2)_{\text{Exp.}}$
$^{11}\text{C}$	20.4 min [22]	$3/2^-$	1.653	-0.7832	-0.964(1)	3.352	3.333(2)*
$^{13}\text{N}$	9.96 min [22]	$1/2^-$	1.685	-0.3326	0.3222(4) *	-----	-----
$^{15}\text{O}$	2.03 min [22]	$1/2^-$	1.713	+0.6377	0.71951(12)*	-----	-----
$^{18}\text{F}$	109.8 min [24]	$1^+$	1.751	+0.8516	-----	-0.706	-----

\*Sign is undetermined

#### 4. Conclusions

The nuclear moments and form factors are important quantities which can accurately reflect the microscopic nuclear structure of nuclei under study. The complete shell model spaces with the appropriate two-body interactions using the HO oscillator single-particle wave functions give a very good description of the available data for the nuclei studied in this work. Core-polarization effects considered in this study for electric moments and Coulomb form factors through effective charges describe the available experimental quadrupole

moment very well, in addition to giving predictions for the Coulomb form factors to be compared with the future experiments on the nuclei considered in this work. Compared with the corresponding stable nuclei in the  $p$ -shell, the form factors of the nuclei considered in this work are consistent with the major trends of the form factors of the corresponded stable nuclei. Good agreements are obtained between the theoretical and experimental magnetic moments.

## References

- [1] R. A. Radhi, A. A. Abdullah, Z. A. Dakhil and N. M. Adeeb, "Core-polarization effects on C2 form factors of  $p$ -shell nuclei," *Nucl. Phys. A*, vol. 696, no. 3-4, pp. 442-452, 2001.
- [2] J. G. L. Booten and A. G. M. van Hees, "Magnetic electron scattering from  $p$ -shell nuclei," *Nucl. Phys. A*, vol. 569, no. 3, pp. 510-522, 1994.
- [3] S. Karataglidis, B. A. Brown, K. Amos and P. J. Dortmass, "Shell model structures of low-lying excited states in  ${}^6\text{Li}$ ," *Phys. Rev. C*, vol. 55, no. 6, pp. 2826-2837, 1997.
- [4] R. A. Radhi, "Microscopic calculations of C2 form factors of  ${}^6\text{Li}$ ," *Nucl. Phys. A* vol. 716, pp.100-106, 2003.
- [5] P. Navratil and B. R. Barrett, "Large-basis shell-model calculations for  $p$ -shell nuclei", *Phys. Rev. C*, vol. 57, no. 6, p. 3119, 1998.
- [6] R. A. Radhi, N. M. Adeeb and A. K. Hashim, "Electro excitations of  ${}^9\text{Be}$  using large-basis shell model," wavefunctions with higher energy configurations," *J. Phys. G: Nucl.Part. Phys.*, vol. 36, p. 105102, 2009.
- [7] R. A. Radhi, Z. A. Dakhil and N.S. Manie, "Microscopic calculations of quadrupole moments in Li and B isotopes," *Eur. Phys. J. A*, vol. 50, article no. 115, 2014.
- [8] R. A. Radhi, G. N. Flaiyh, E. M. Raheem, "Electric Quadrupole Transitions of Some Even-Even Neon Isotopes," *Iraqi Journal of Science*, vol. 56, no. 2A, pp. 1047-1060, 2015.
- [9] R. A.Radhi, Ali A. Alzubadi, Eman M. Rashed, " Shell model calculations of inelastic electron scattering for positive and negative parity states in  ${}^{19}\text{F}$ ," *Nucl. Phys. A*, vol. 947, pp.12-25, 2016.
- [10] R. A. Radhi, A. H. Ali, "Microscopic calculations of effective charges and quadrupole transition rates in Si, S and Ar isotopes," *Iraqi Journal of Science*, vol. 57, no. 3B, pp.1999-2013, 2016.
- [11] R.A. Radhi, Ali A. Alzubadi, Ahmed H. Ali, "Calculations of the Quadrupole Moments for Some Nitrogen Isotopes in  $p$  and  $psd$  Shell Model Spaces Using Different Effective Charges," *Iraqi Journal of Science*, vol. 58, no. 2B, pp. 878-883, 2017.
- [12] Ali A. Alzubadi, R. A. Radhi, and Noori S. Manie, "Shell model and Hartree-Fock calculations of longitudinal and transverse electroexcitation of positive and negative parity states in  ${}^{17}\text{O}$ ," *Phys. Rev. C*, vol. 97, no. 2, p. 024316, 2018.
- [13] R. A. Radhi, Ali A. Alzubadi, and A. H. Ali, "Magnetic dipole moments, electric quadrupole moments, and electron scattering form factors of neutron-rich  $sd$ -  $pf$  cross-shell nuclei," *Phys. Rev. C*, vol. 97, no. 6, p. 064312, 2018.
- [14] P. J. Brussaard and P. W. M. Glaudemans, "Shell Model Applications in Nuclear Spectroscopy," North Holland Publishing Company, Amsterdam, 1977.
- [15] B. A. Brown, B. H. Wildenthal, C. F. Williamson, F. N. Rad, S. Kowalski, H. Crannell, and J. T. O'Brien, "Shell-model analysis of high-resolution data for elastic and inelastic electron scattering on  ${}^{19}\text{F}$ ," *Phys. Rev. C*, vol. 32, pp. 1127-1156, 1985.
- [16] S. Cohen, D. Kurath, "Effective interactions for the  $1p$  shell," *Nucl. Phys.*, vol. 73, pp.1- 24, 1965.
- [17] B. Alex Brown and W. A. Richter, "New "USD" Hamiltonians for the  $sd$  shell," *Phys. Rev. C*, vol. 74, p. 034315, 2006.
- [18] NuShellX, W.D.M. Rae, "The Shell-Model Code NuShellX@MSU", <http://www.garsington.eclipse.co.uk>.
- [19] B. A. Brown, R. Radhi, and B. H. Wildenthal, "Electric quadrupole and Hexadecupole Nuclear Excitations from the perspectives of electron scattering and modern shell-model theory," *Phys. Rep.*, vol. 101, no. 5, pp.313-358, 1983.

- [20] W. A. Richter, S. Mkhize, and B. Alex Brown, “sd-shell observables for the USDA and USDB Hamiltonians,” *Phys. Rev. C*, vol. 78, p. 064302, 2008.
- [21] Carlotta Taddei and Victor W. Pike, “Carbon monoxide: advance in production and application to PET radiotracer development over the past 15 years,” *EJNMMI Radiopharmacy and Chemistry*, vol. 4, article no. 25, pp.1-31, 2019.
- [22] N. J. Stone, “Table of Nuclear Magnetic Dipole and Electric Quadrupole Moments”, Oxford Physics, Clarendon Laboratory, Parks Road, Oxford U.K. OX1 3PU and Department of Physics and Astronomy, University of Tennessee, Knoxville, USA, TN 37996-1200, INDC International Nuclear Data Committee, IAEA Nuclear Data Section Vienna International Centre, P.O. Box 100, 1400 Vienna, Austria, 2014.
- [23] R.N. Krasikova, O.S. Fedorova , M.V. Korsakov , B. Landmeier, Bennington, M.S. Berridge, “Improved [13N] ammonia yield from the proton irradiation of water using methane gas,” *Applied Radiation and Isotopes*, vol. 51, no. 4, pp.395-401, 1999.
- [24] Mian M. Alauddin, “Positron emission tomography (PET) imaging with <sup>18</sup>F-based radiotracers,” *Am J Nucl Med Imaging*, vol. 2, no. 1, pp. 55-76, 2012.